Catalysis Today 164 (2011) 282–287

Contents lists available at ScienceDirect

Catalysis Today

journal homepage: www.elsevier.com/locate/cattod

Ru-based catalysts for CO selective methanation reaction in H_2-rich gases

Petar Djinović[a,b], Camilla Galletti[a,*], Stefania Specchia[a], Vito Specchia[a]

[a] Department of Materials Science and Chemical Engineering, Politecnico di Torino, Corso Duca degli Abruzzi 24, 10129 Torino, Italy
[b] Laboratory for Catalysis and Chemical Reaction Engineering, National Institute of Chemistry, Hajdrihova 19, SI 1001 Ljubljana, Slovenia

ARTICLE INFO

Article history:
Received 30 June 2010
Received in revised form 29 October 2010
Accepted 2 November 2010
Available online 3 December 2010

Keywords:
H_2 clean-up
Selective methanation
Ru-based catalysts
Ceria
Alumina

ABSTRACT

Even traces of CO in the hydrogen-rich gas fed to PEM-FCs can poison the platinum anode electro-catalyst and dramatically decrease the stack power. The CO selective methanation (CO-SMET) process seems to be a good alternative to the CO preferential oxidation (CO-PROX) one for PEM-FCs applications to vehicles, boats, yachts and residential co-generators, as a CO-SMET reactor is inherently easier to control than the CO-PROX one. The present paper deals with the study on complete removal of CO in H_2-rich gas stream from a reforming process through CO-SMET over Ru-based catalysts supported on Al_2O_3 and CeO_2 carriers. All the catalysts, with Ru load of 1%, 3% and 5%, were prepared by a conventional impregnation method, using two different Ru precursors, chloride and nitrate, and their CO removal performance was determined at the powder level in a fixed bed micro reactor. The Al_2O_3 carrier exhibited performances better than the CeO_2 one, in particular when Ru was deposited from $RuCl_3$ precursor. The best performance was obtained with 5% Ru–Al_2O_3_Cl as the temperature range of complete CO conversion with acceptably low levels of CO_2 methanation (≤50% of CO molar methanation) was the widest.

1. Introduction

Automotive exhaust is currently one of the major pollution sources. As a pollution-free and energy-saving power supply for electric vehicles, the proton exchange membrane fuel cells (PEM-FCs) are one of the best candidates because of their high energy conversion efficiency (50–70%) and zero or nearly zero emissions. Hydrogen is the ideal fuels for PEM-FCs [1,2]. However, due to lack of H_2 distribution nets, H_2-rich gas streams obtained from hydrocarbon feedstocks reforming and suitably cleaned-up from CO are they too PEM-FCs ideal fuels [1,2].

One of the major problems for the application of low temperature (LT) PEM-FCs as power source for electrically operated vehicles is the delivery of "nearly-CO-free" feed gas, which becomes problematic whenever H_2 is generated from fuels. As the FC anodes can be poisoned even by trace impurities of CO, this gas has to be removed to a concentration below 50 ppm for the state-of-art Pt–Ru anode electro-catalysts [3–5] and below 10 ppmv for Pt anode electro-catalysts [6–8].

However, in order to increase the H_2 rate in the reformate gas, for PEM-FCs applications on vehicles, residential co-generators and portable devices, the clean-up process starts with a water gas shift (WGS) step from which the residual CO concentration is in the 0.5–1% range. As the final clean-up step, a reasonable selection, because of the limited available spaces on board vehicles and low operating pressures, may be done between the preferential CO oxidation (CO-PROX) and the selective CO methanation (CO-SMET).

The CO-PROX has so far been extensively studied since it is somehow reliable to remove CO down to 10 ppmv by suitably raising the oxygen feeding rate. Nonetheless, the process target of high power efficiency requires a closely controlled low O_2 supply to keep the possibly lowest H_2 parallel oxidation; moreover, a generally sufficient large range of working temperatures is required too for safe process controllability. This, while making the method costly and complex (suitable control apparatuses are necessary to adapt the oxygen supplies to unavoidable system fluctuations), obviously increases the difficulty of its application to low-power PEM-FCs where very small oxidant flow rates have to be provided by the use of well-refined expensive dosing systems. Consequently, it should be challenging to apply the CO-PROX process to the on-commercializing small PEM-FCs for residential and portable uses.

Without any additional reactant required, the selective CO methanation (CO-SMET), can avoid the above-mentioned CO-PROX shortcomings. Furthermore, CO and CO_2 methanation (Eqs. (1) and (2), the second reaction obviously possible due to the abundant presence of CO_2 in the reformate gas) are less exothermic than the CO and H_2 oxidations (Eqs. (3) and (4)). Thus, the CO-SMET process is inherently easier controllable than the CO-PROX one.

$$CO + 3H_2 \rightarrow CH_4 + H_2O \quad \text{CO-SMET} \quad \Delta H^{\circ}_{298\,^{\circ}C} = -206.2\ \text{kJ mol}^{-1} \tag{1}$$

$$CO_2 + 4H_2 \rightarrow CH_4 + 2H_2O \quad \text{CO}_2\text{-MET} \quad \Delta H^{\circ}_{298\,^{\circ}C} = -164.9\ \text{kJ mol}^{-1} \tag{2}$$

* Corresponding author. Tel.: +39 011 0904699.
E-mail address: camilla.galletti@polito.it (C. Galletti).

0920-5861/$ – see front matter © 2010 Elsevier B.V. All rights reserved.
doi:10.1016/j.cattod.2010.11.007

$$CO + (1/2)2O_2 \rightarrow CO_2 \quad \text{CO-PROX} \quad \Delta H^{\circ}_{298\,^{\circ}C} = -283.6\,\text{kJ mol}^{-1} \tag{3}$$

$$H_2 + (1/2)O_2 \rightarrow H_2O \quad \text{Hy-OX} \quad \Delta H^{\circ}_{298\,^{\circ}C} = -243.5\,\text{kJ mol}^{-1} \tag{4}$$

Eq. (1) shows that the removal of 1 mol CO via methanation requires 3 mol of H_2. Of these, 2 mol, together with carbon, are restored in the CH_4 product, which can be reused after PEM-FCs reactions through recirculating the anode stack off-gas into the FPU as a fuel to be burnt giving high temperature flue gases for the FPU heating necessities, so with a more interesting utilization from a thermodynamic point of view.

A PEM-FC system, in general, has to be equipped with an off-gas re-circulation line to recover the unreacted H_2 that may reach 15–20% of its original fed rate [9–13]. Hence, for CO-SMET the actual net H_2 loss into water should be 1 mol for 1 mol of removed CO, if the methanation selectivity towards CO is 100% (three for methanation minus two recovered in producing heat from CH_4 burn-out). For the CO-PROX there is theoretically no H_2 loss if the O_2 selectivity towards CO is equal to 1 (based on Eq. (3)). This theoretical result, however, is hardly possible to be reached in practice over commercial catalysts, but none is willing to risk the stack safety by operating at an oxidation stoichiometry in the CO-PROX reactor λ = O/CO equal to 1.0 (v/v), even if the catalyst could allow, also considering that actual PEM-FC stacks fluctuate intrinsically. Therefore, some O_2 excess allows a safer reactor management, but, as a consequence, some H_2 loss, via Eq. (4), surely exists in practical CO-PROX reactors. This loss, based on literature reports [14,15], should be at least 1–2 mol of H_2 for 1-mol CO removal because actual CO-PROX reactors run generally at λ values of 2–3 (v/v) [16].

By considering pros and cons, the CO-SMET process can be proposed as a promising route to remove CO in the reformate stream and as an alternative process to CO-PROX in FPUs for mobile and residential PEM-FCs applications.

Methanation of CO over various carried metal catalysts such as Co, Ni, Ru, Rh etc., has been widely investigated from the viewpoint of synthesizing CH_4 from syngas [17–21], and recently also from a viewpoint of residual CO removal for PEM-FC applications [22–30].

After a previous study on Ru-based catalysts on different carriers [30] and on the basis of literature results on Ru–γAl_2O_3 catalysts [31], which shown a not satisfactory performance for CO-SMET, in this paper Ru-based catalysts on Al_2O_3 and CeO_2 as carriers were investigated at the powder level as concerns the effect of the Ru precursor and the active metal load on both the selective methanation of CO in a reformate gas and the temperature range width of CO complete conversion with acceptably low CO_2 methanation.

2. Experimental

CeO_2 and Al_2O_3 supports were produced by solution combustion synthesis (SCS) method at 600 °C [32,33]. Obtained oxides were ground in a mortar and calcined in still air at 650 °C for 2 h. The active metal Ru was deposited by incipient wetness impregnation (IWI) starting from two different precursors, $RuCl_3 \cdot xH_2O$ and $Ru(NO)(NO_3)_3$ dissolved in distilled water; the solution was added drop by drop over the carrier meanwhile thoroughly mixing. The mixture was then placed to dry in oven at 200 °C. Next, the powdered catalysts were calcinated 2 h at 350 °C in still air and ground again. Three Ru loads were prepared: 1%, 3%, and 5% by weight.

XRD analysis (Philips PW1710 apparatus equipped with a monochromator for the Cu Kα radiation) was performed on the freshly prepared catalysts to verify their composition. The specific surface area of the Ru-supported catalysts was measured via N_2 by the BET method (Micromeritics ASAP 2020 C apparatus). The morphology of the as prepared catalysts was additionally examined by field emission scanning electron microscopy (FESEM Leo Supra 40 apparatus) with energy dispersive X-ray analysis (Oxford Instruments Inca EDX apparatus).

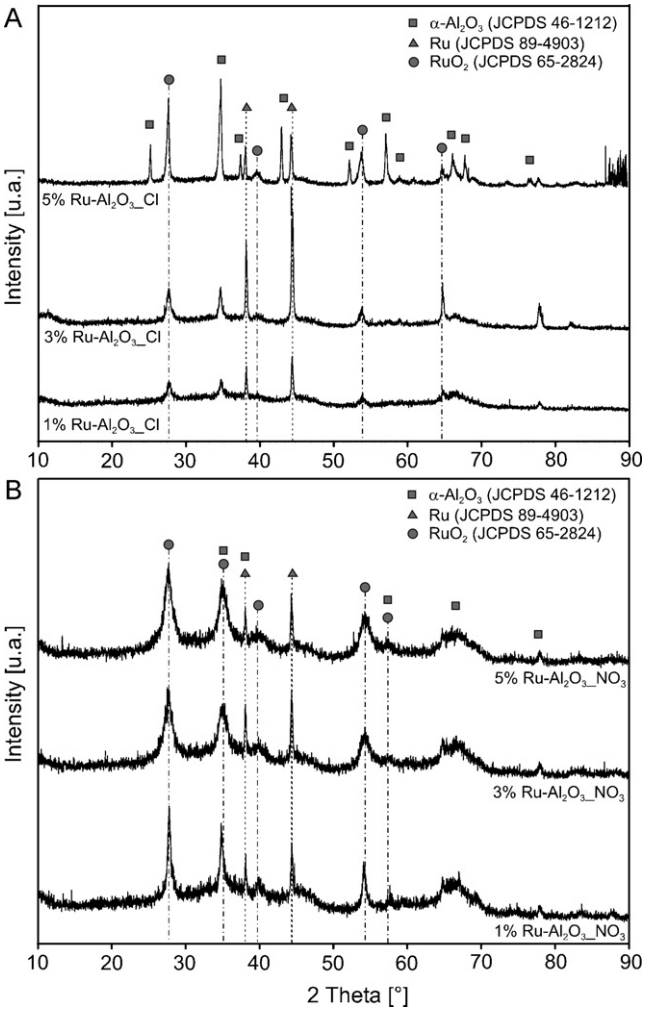

Fig. 1. XRD spectra for Ru catalysts supported on Al_2O_3, prepared starting from chloride (A) and nitrate (B) precursor.

A fixed bed micro-reactor (a quartz tube of 4 mm I.D.), heated up by a PID regulated oven and containing 0.3 g of catalyst in powder, diluted with 0.5 g of SiO_2, held in place by flocks of quartz wool, was used for the CO-SMET reaction. A K-type thermocouple was inserted into the reactor to measure the temperature of the catalytic bed. The inlet gas was fed at a flow rate of 100 N ml min^{-1} (weight space velocity WSV = 0.33 N l min^{-1} g_{cat}^{-1}) and with the following composition (vol.%): 0.56% CO, 42.2% H_2, 21.7% CO_2 and N_2 as balance (standard rate and standard feed gas composition employed in our research group for the catalysts activity screening). This composition (N_2 apart) is representative of the outlet stream from a typical WGS process downstream a gasoline auto-thermal reformer. The outlet gas stream from the CO-SMET micro-reactor was analyzed through a micro gas-chromatograph (Varian CP-4900) equipped with a thermal conductivity detector. The CO detection limit was 2 ppmv. The CO conversion (ξ_{CO}) and CH_4 formation were determined in the 150–450 °C range. Before tests, catalysts were activated in 100% H_2 flow at 250 °C for 2 h.

3. Results and discussion

A preliminary characterization of the as-prepared Ru-based catalysts was carried out with XRD (Figs. 1 and 2) and BET specific surface area (Table 1).

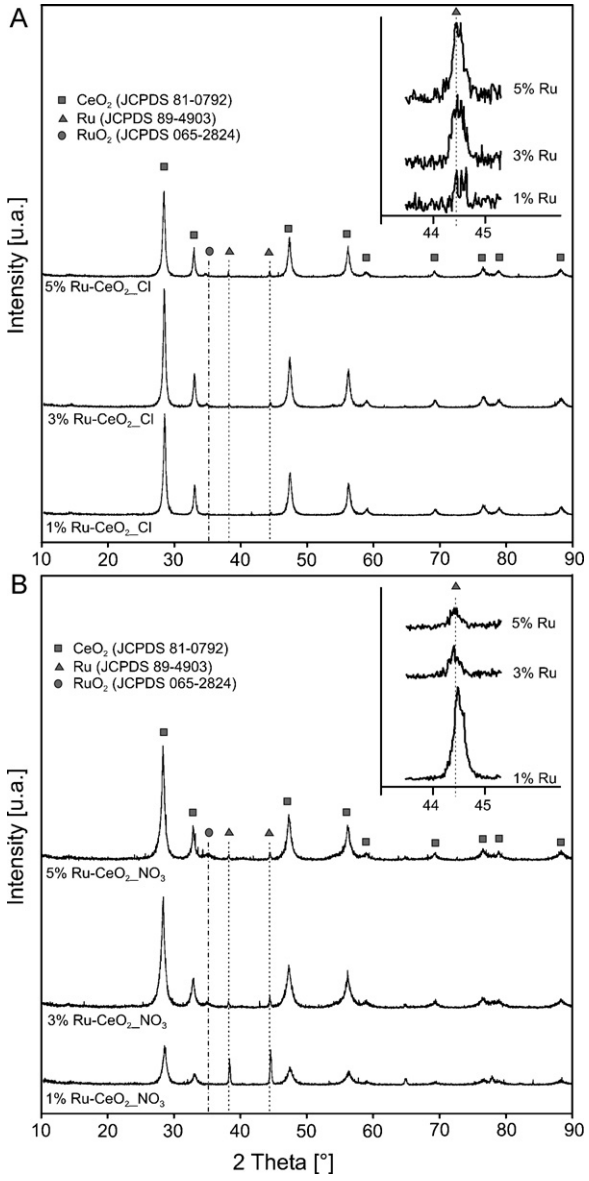

Fig. 2. XRD spectra for Ru catalysts supported on CeO_2, prepared starting from chloride (A) and nitrate (B) precursor.

From the XRD spectra of the Ru–Al_2O_3-based catalysts (see Fig. 1), Al_2O_3 carrier appeared more crystallized (as α phase) when Ru was deposited starting by chloride precursor, whereas when nitrate precursor was used, the presence of an amorphous form was enlightened. Ru and RuO_2 peaks were visible for all the Ru–Al_2O_3_Cl and Ru–Al_2O_3_NO_3 catalysts. From the XRD spectra of the Ru–CeO_2-based catalysts (see Fig. 2), CeO_2 appeared well crystallized with thinner peaks, Ru peaks were very small and visible only by suitably enlarging the diagrams at 2θ angle of 44.4° (see the inserts in Fig. 2).

Table 1
Characterization of Ru-based catalysts.

Catalyst	BET specific surface area [$m^2\ g^{-1}$]	Ru crystallite size [nm]
1% Ru–CeO_2_Cl	19.6	32.7
3% Ru–CeO_2_Cl	20.2	32.5
5% Ru–CeO_2_Cl	19.2	31.6
1% Ru–CeO_2_NO_3	11.9	31.1
3% Ru–CeO_2_NO_3	12.4	33.5
5% Ru–CeO_2_NO_3	12.8	32.0
1% Ru–Al_2O_3_Cl	173	31.8
3% Ru–Al_2O_3_Cl	160	30.8
5% Ru–Al_2O_3_Cl	155	33.3
1% Ru–Al_2O_3_NO_3	239	31.9
3% Ru–Al_2O_3_NO_3	233	31.3
5% Ru–Al_2O_3_NO_3	229	31.4

Approximate Ru metal crystallite sizes over all the carriers were estimated using the data from the XRD patterns broadening and the Scherrer formula (Eq. (5)):

$$L = \frac{0.9 \cdot \lambda}{B_{2\theta} \cdot \cos 2\theta} \quad (5)$$

where L is the crystallite size, λ is the wavelength of the filament used in the XRD item (equal to 1.54 Å in our case), $B_{2\theta}$ is the line broadening at half the maximum intensity (FWHM) in radians, and 2θ is the Bragg angle [34]. The calculated data are listed in Table 1.

BET s.s.a. values are also listed in Table 1: different results were obtained when using different Ru precursors for deposition, whereas Ru load did not influence particularly the BET values.

FESEM investigation completed the physical characterization of the as-prepared catalysts. In Fig. 3, 3% Ru–Al_2O_3 prepared starting from Ru chloride precursor was compared to the one synthesized with nitrate precursor. Active metal particles with different shape were obtained: with chloride precursor, Ru particles appeared as needles grown on the carrier surface, whereas with nitrate precursor a layer of small Ru particles coated the carrier. The EDX analysis performed on the different morphological areas of the samples allowed identifying Ru: the obtained results are reported in the FESEM pictures in Fig. 3, as analyzed zone areas and atomic Ru/Al ratio. It is visible that the needle-shaped particles (Ru–Al_2O_3_Cl catalyst, Fig. 3A) and the small particles (Ru–Al_2O_3_NO_3 catalyst, Fig. 3B) corresponded to metallic Ru; on the contrary, in the other areas Ru was not identified or was present in very limited amount.

For the Ru–Al_2O_3 catalysts prepared from nitrosyl nitrate precursor, Ru particle dimensions of 25–35 nm detected by FESEM, were in agreement with the crystallite sizes determined from XRD spectra, according to Scherrer calculation. Therefore, no crystal agglomeration seemed to take place on Ru–Al_2O_3_NO_3 catalysts. On the other hand, Ru particles over Ru–Al_2O_3 from $RuCl_3$, as observable from FESEM micrographs, were roughly 10 times larger, compared to those calculated XRD spectra. This discrepancy indicated that the particles observed by FESEM were actually agglomerates of crystallites, whose size was identified with XRD. A higher agglomeration tendency of Ru–Al_2O_3_Cl catalysts, compared to Ru–Al_2O_3_NO_3 samples, was presumably caused by the different chemical nature of the Ru precursor used. Same results were obtained for ceria supported catalyst (micrographs not shown here).

A preliminary screening of the performance of Ru-based catalysts on CeO_2 and γAl_2O_3 supports was carried out in terms of CO conversion (ξ_{CO}). Figs. 4 and 5 show the effect of both the different Ru precursors and the active metal load on the catalytic performance of Ru–CeO_2 and Ru–Al_2O_3 catalysts, respectively.

All the Ru–CeO_2 catalysts prepared with nitrate Ru precursor reached complete ξ_{CO}: the largest temperature range, ΔT, of complete ξ_{CO} was obtained with 3% Ru on ceria: ΔT equal to 203–251 °C. The ΔT became less large for the catalyst with higher Ru load (5%), whereas, decreasing the load to 1%, the complete CO conversion was obtained only at 235 °C. When the metal deposition was carried out starting from chloride precursor, the catalysts performance slightly worsened: in particular with 1% Ru–CeO_2 complete CO conversion was not achieved (maximum conversion ξ_{COmax} = 96%). For all the Ru–CeO_2 catalysts, the obtained ΔT values are listed in the upper part of Table 2.

As concerns the Ru–Al_2O_3 catalysts, the ξ_{CO} was positively affected increasing Ru load: in fact, on the whole, Ru–Al_2O_3 catalysts, compared with ceria-supported ones, maintained complete

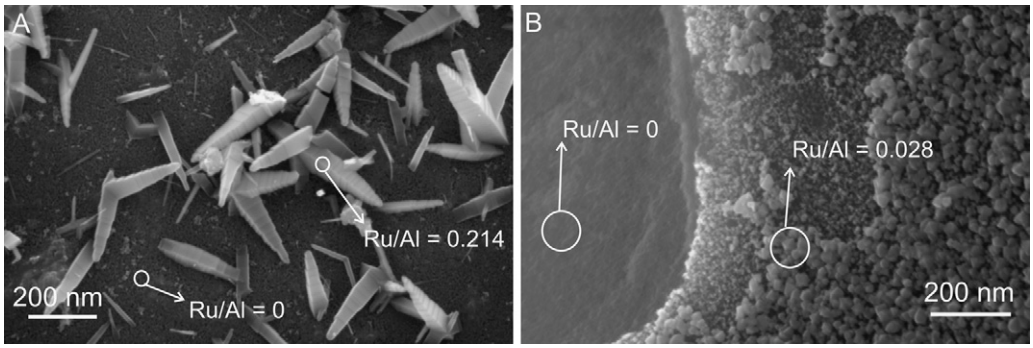

Fig. 3. FESEM images of 3% Ru–Al_2O_3 prepared with chloride (A) and nitrate (B) precursor. Ru/Al atomic ratios from EDX analysis are shown.

conversion for wider temperature ranges, but the average operating temperatures for $\xi_{CO} = 1$ shifted at slightly higher values. For all the Ru–Al_2O_3 catalysts, the ΔT values are reported in the lower part of Table 2.

In any cases, for all the prepared catalysts, after the complete conversion, the CO concentration increased again (and ξ_{CO} obviously decreased) by increasing the temperature. This could be probably due to the reverse water gas shift reaction R-WGS (Eq. (6)), thermodynamically and kinetically favoured at higher temperature:

$$CO_2 + H_2 \rightarrow CO + H_2O \quad \text{R-WGS} \quad \Delta H_{298\,^\circ C} = +41.2\,\text{kJ mol}^{-1} \quad (6)$$

Moreover, also by the experimental results reported in the paper [35], related to both CO and CO_2 methanation over 0.5–5% Ru–alumina catalysts, seem to confirm the low CO conversion at high temperature. Panagiotopoulou et al. [35], in fact, using a fixed bed reactor fed with a molar composition similar to that employed in this study ([35]: 1% CO, 50% H_2, 15% CO_2 and He as balance; this study: 0.56% CO, 42.2% H_2, 21.7% CO_2 and N_2 as balance) obtained

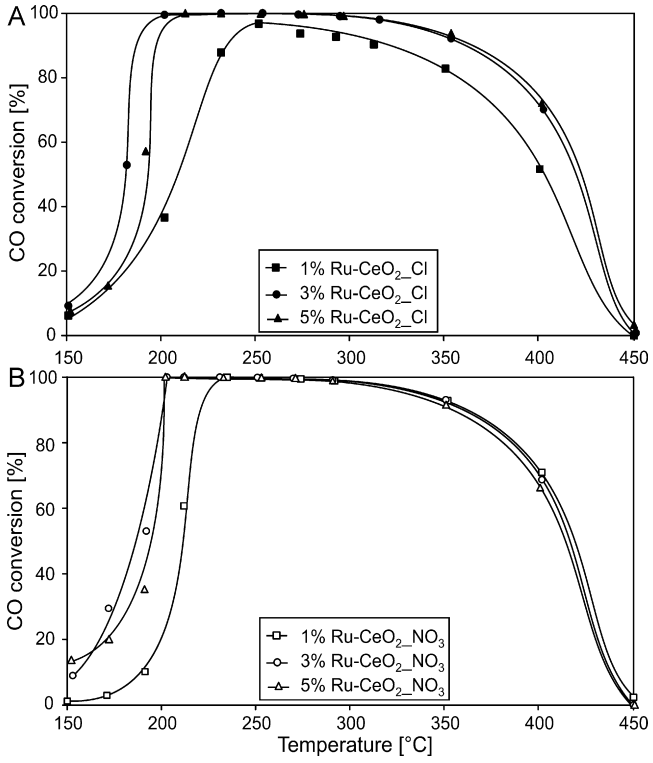

Fig. 4. CO conversion ξ_{CO} vs. T for Ru–CeO_2 catalysts prepared starting from chloride (A) and nitrate (B) precursor (standard feed gas composition; WSV = 0.33 N l min^{-1} g_{cat}^{-1}).

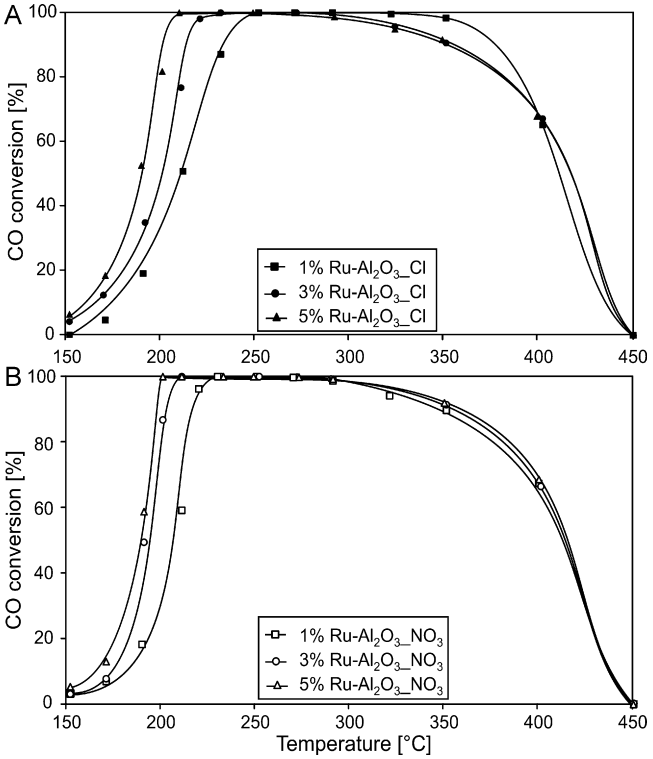

Fig. 5. CO conversion ξ_{CO} vs. T for Ru–Al_2O_3 catalysts prepared starting from chloride (A) and nitrate (B) precursor (standard feed gas composition; WSV = 0.33 N l min^{-1} g_{cat}^{-1}).

negative values of CO conversion (till −90%) at temperature higher than 370 °C. The authors claimed RWGS as responsible of CO production in such a quantity till to overcome the fed one. Moreover, they presented also the CO and CO_2 turnover frequencies TOFs: at

Table 2
Temperature conditions for $\xi_{CO} = 1$ for Ru–CeO_2 and Ru–Al_2O_3 catalysts.

Catalyst	Min T value [°C]	Max T value [°C]	ΔT range [°C]	Average T value [°C]
1% Ru–CeO_2_Cl	–	–	–	–
3% Ru–CeO_2_Cl	232	254	22	243
5% Ru–CeO_2_Cl	213	253	40	233
1% Ru–CeO_2_NO_3	235	235	0	235
3% Ru–CeO_2_NO_3	203	251	48	227
5% Ru–CeO_2_NO_3	202	233	31	217.5
1% Ru–Al_2O_3_Cl	252	322	70	287
3% Ru–Al_2O_3_Cl	232	291	59	261.5
5% Ru–Al_2O_3_Cl	210	272	62	241
1% Ru–Al_2O_3_NO_3	230	270	40	250
3% Ru–Al_2O_3_NO_3	211	272	61	241.5
5% Ru–Al_2O_3_NO_3	201	273	72	237

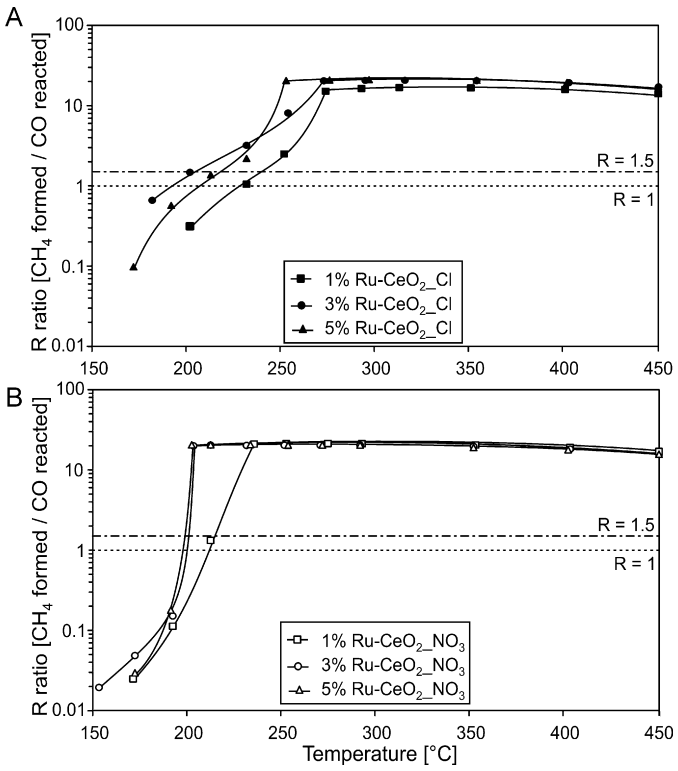

Fig. 6. R vs. T for Ru–CeO_2 catalysts prepared with chloride (A) and nitrate (B) precursor.

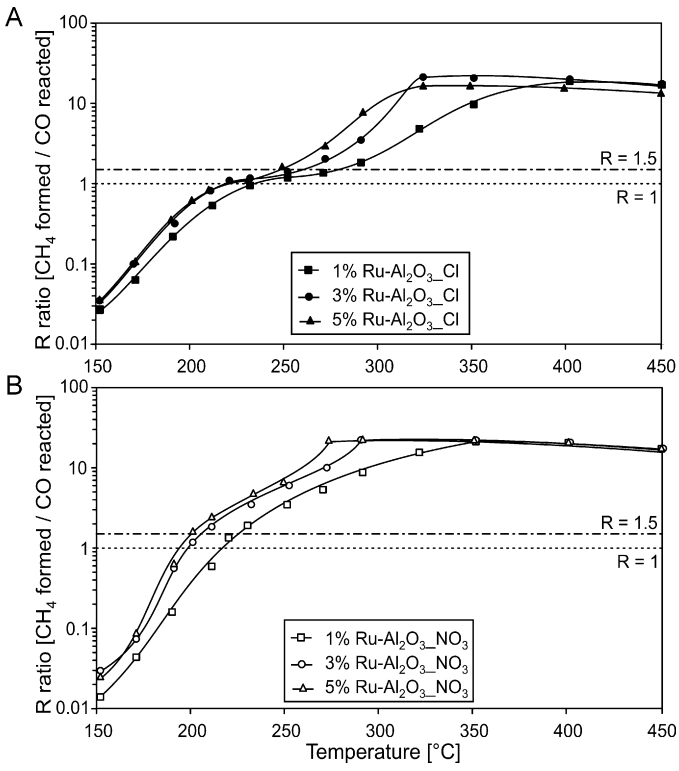

Fig. 7. R vs. T for Ru–Al_2O_3 catalysts prepared with chloride (A) and nitrate (B) precursor.

about 300 °C the two TOFs were equal, but at lower temperature the TOF of CO-MET was higher than the one for CO_2-MET and at higher temperature the TOF of CO_2-MET resulted higher than the one for CO-MET. By extrapolating the TOF data in [35] at 400 °C (where from our results the CO conversion resulted to be very low), CO_2 methanation TOF was about 50 times higher than that of CO methanation. Therefore, both the experimental findings could justify the low CO-MET conversion obtained at high temperatures.

As CO and CO_2 methanation are in competition, the outlet CH_4 rate derived also from CO_2 methanation (Eq. (2)); the moles of methane obtained form CO_2 were calculated and compared to the ones from CO methanation through the parameter R, equal to the ratio: mole formed CH_4/mole reacted CO. $R = 1$, simultaneously with $\xi_{CO} = 1$, indicates that the formed CH_4 derives totally from the reaction of CO with H_2 (CO methanation selectivity $\sigma_{CO} = 1$), whereas $R > 1$ with $\xi_{CO} \leq 1$ is an index of a certain degree of CO_2 methanation ($\sigma_{CO} < 1$).

The calculated R values for all the CeO_2 and Al_2O_3 supported catalysts are shown in Figs. 6 and 7, respectively. With the goal to determine an optimum working temperature range (namely, ΔT°), characterized by CO complete conversions, $\xi_{CO} = 1$ and, at the same time, an acceptably low maximum R value (with R_{max} assumed equal to 1.5), the ΔT° ranges matching simultaneously $\xi_{CO} = 1$ and $R \leq R_{max}$ were evaluated.

Concerning ceria supported catalytic materials, only for 5% Ru–CeO_2_Cl catalyst a ΔT° value was obtained: $\Delta T^\circ = 213–217 = 4$ °C, anyway, a very narrow range for the reactor controllability. For the other ceria based catalysts no overlapping between the temperature range of $\xi_{CO} = 1$ and the one of $R \leq R_{max}$ was found. The results picture for alumina supported catalysts was more interesting, showing satisfactory ΔT° values, which are reported in Table 3. Analysing these results, a reasonable overlapping of the temperature range of $\xi_{CO} = 1$ with the one of R lower than the assumed R_{max} was obtained only for the Ru–γAl_2O_3 catalysts prepared with the chloride precursor, in particular for 5% Ru–γAl_2O_3 (210–244 °C, $\Delta T^\circ = 34$ °C). On the contrary, using the nitrate precursor, the complete CO conversion was obtained at R values larger than R_{max}, so no temperature range overlapping was possible ($\Delta T^\circ = 0$).

Table 3
ΔT° values for Ru–Al_2O_3 catalysts.

Catalyst	$\xi_{CO} = 1$ and $R \leq R_{max}$
1% Ru–Al_2O_3_Cl	$\Delta T^\circ = 252 – 276 = 24$ °C
3% Ru–Al_2O_3_Cl	$\Delta T^\circ = 232 – 253 = 21$ °C
5% Ru–Al_2O_3_Cl	$\Delta T^\circ = 210 – 244 = 34$ °C
1% Ru–Al_2O_3_NO_3	$\Delta T^\circ = 0$ °C
3% Ru–Al_2O_3_NO_3	$\Delta T^\circ = 0$ °C
5% Ru–Al_2O_3_NO_3	$\Delta T^\circ = 0$ °C

Therefore, the alumina based Ru catalysts demonstrated to be more selective towards CO methanation when Ru was deposited from $RuCl_3$ precursor.

By comparing the obtained catalysts ΔT° working temperature ranges with the usual temperature range of the reformate gas leaving the WGS process (220–250 °C), a methanation reactor containing the 3% Ru–Al_2O_3 or 5% Ru–Al_2O_3 catalysts could be directly fed with the gas stream from the WGS reactor without any heat exchange. On the contrary, by using the 1% Ru–Al_2O_3 catalyst a pre-heating operation could be necessary, rendering in this way also more complex the plant scheme of the H_2-gas clean-up section of the FPU (not only for one more heat exchanger to be installed, as much, where to find the properly hot stream for pre-heating the methanator feed), moreover, with a new heat exchanger not so easy to be managed (a pre-heating range of the methanator feed of about 15–45 °C).

4. Conclusions

The complete removal of CO from H_2-rich gas stream (reformate gas from WGS process) by methanation was investigated over Ru-

based powder catalysts supported on CeO_2 and γAl_2O_3. Different Ru loads were deposited on both the carriers employing two different precursors: $Ru(NO)(NO_3)_3$ and $RuCl_3{\cdot}xH_2O$.

The prepared catalysts performance in the powder status was evaluated in a fixed bed micro reactor in terms of CO conversion, ξ_{CO}, and the parameter $R = CH_4$ formed/CO reacted. R values higher than $R_{max} = 1.5$ were not considered since characteristic of a too large H_2 consumption by CO_2 methanation. A preliminary screening showed the better performance of Al_2O_3 carrier compared to CeO_2: for catalysts supported on ceria, only for 5% Ru–CeO_2_Cl the ΔT° working temperature range (characterized by $\xi_{CO} = 1$ and $R \leq R_{max}$) resulted to exist and to be: $\Delta T^\circ = 213–217 = 4\,^\circ C$, anyway, a very small value for a safe reactor temperature controllability.

Regarding alumina catalysts, acceptable ΔT° values resulted for all the catalysts prepared starting from chloride precursor: 1% Ru–γAl_2O_3 ($\Delta T^\circ = 252–276 = 24\,^\circ C$), 3% Ru–$\gamma Al_2O_3$ ($\Delta T^\circ = 232–253 = 21\,^\circ C$) and 5% Ru–$\gamma Al_2O_3$ ($\Delta T^\circ = 210–244\,^\circ C = 34\,^\circ C$). In particular, 5% Ru–$Al_2O_3$_Cl catalyst showed the best overall performance: in the working conditions of industrial interest, ΔT° presented a width quite suitable for the reactor control and, moreover, compatible with the temperature of the stream coming out from the WGS reactor, so without the need of a further heat exchanger to adjust the CO-SMET reactor inlet temperature.

On the contrary, for the catalysts prepared using nitrate precursor no overlapping was found between the temperature range of $\xi_{CO} = 1$ and the one of $R \leq R_{max}$, so ΔT° resulted to be zero.

References

[1] A.K. Shukla, A.S. Aricò, V. Antonucci, Renew. Sust. Energy Rev. 5 (2001) 137–155.
[2] L. Carrette, K.A. Friedrich, U. Stimming, Fuel Cells 1 (2001) 5–39.
[3] N. Fujiwara, K. Yasuda, T. Ioroi, Z. Siroma, Electrochim. Acta 47 (2002) 4079–4084.
[4] C.G. Farrell, C.L. Gardner, M. Ternan, J. Power Sources 171 (2007) 282–293.
[5] X. Cheng, Z. Shi, N. Glass, L. Zhang, J. Zhang, D. Song, Z.-S. Liu, H. Wang, J. Shen, J. Power Sources 165 (2007) 739–756.
[6] J. Divisek, H.-F. Oetjen, V. Peinecke, V.M. Schmidt, U. Stimming, Electrochim. Acta 43 (1998) 3811–3815.
[7] E. Passalacqua, F. Lufrano, G. Squadrito, A. Patti, L. Giorni, J. New Mater. Electrochem. Syst. 3 (2000) 141–146.
[8] B.J. Bowers, J.L. Zhao, M. Ruffo, R. Khan, D. Dattatraya, N. Dushman, J.-C. Beziat, F. Boudjemaa, Int. J. Hydrogen Energy 32 (2007) 1437–1442.
[9] P.G. Gray, M.I. Petch, Platinum Met. Rev. 44 (2000) 108–111.
[10] G.A. Petrachi, G. Negro, S. Specchia, G. Saracco, P.L. Maffettone, V. Specchia, Ind. Eng. Chem. Res. 44 (2005) 9422–9430.
[11] A. Cutillo, S. Specchia, M. Antonini, G. Saracco, V. Specchia, J. Power Sources 154 (2006) 379–385.
[12] S. Specchia, F.W.A. Tillemans, P.F. van den Oosterkamp, G. Saracco, J. Power Sources 145 (2005) 683–690.
[13] S. Specchia, A. Cutillo, G. Saracco, V. Specchia, Ind. Eng. Chem. Res. 45 (2006) 5298–5307.
[14] S.H. Lee, J. Han, K.-Y. Lee, J. Power Sources 109 (2002) 394–402.
[15] G. Xu, X. Chen, K. Honda, Z.-G. Zhang, AIChE J. 50 (2004) 2467–2480.
[16] G. Xu, X. Chen, Z.G. Zhang, Chem. Eng. J. 121 (2006) 97–100.
[17] N.W. Gupta, V.S. Kamble, K.A. Rao, R.M. Iyer, J. Catal. 60 (1979) 57–67.
[18] G.A. Somorjai, Catal. Rev.: Sci. Eng. 23 (1981) 189–202.
[19] K.B. Kester, E. Zagli, J.L. Falconer, Appl. Catal. 22 (1986) 311–319.
[20] W.J. Wang, Y.W. Chen, Appl. Catal. 77 (1991) 21–36.
[21] Y. Borodko, G.A. Somorjai, Appl. Catal. A: Gen. 186 (1999) 355–362.
[22] S. Takenaka, K. Kawashima, H. Matsune, M. Kishida, Appl. Catal. A: Gen. 321 (2007) 165–174.
[23] O. Görke, P. Pfeifer, K. Schubert, Catal. Today 110 (2005) 132–139.
[24] M.S. Batista, E.I. Santiago, E.M. Assaf, E.A. Ticianelli, J. Power Sources 145 (2005) 50–54.
[25] M.B.I. Choudhury, S. Ahmed, M.A. Shalabi, T. Inui, Appl. Catal. A: Gen. 314 (2006) 47–53.
[26] Y. Men, G. Kolb, R. Zapf, V. Hessel, H. Löwe, Catal. Today 125 (2007) 81–87.
[27] M. Krämer, M. Duisberg, K. Stöwe, W.F. Maier, J. Catal. 251 (2007) 410–422.
[28] R.A. Dagle, Y. Wang, G.-G. Xia, J.J. Strohm, J. Holladay, D.R. Palo, Appl. Catal. A: Gen. 326 (2007) 213–218.
[29] Z.-G. Zhang, G. Xu, Catal. Commun. 8 (2007) 953–956.
[30] C. Galletti, S. Specchia, G. Saracco, V. Specchia, Int. J. Chem. React. Eng. 5 (2007) A110.
[31] S. Takenaka, T. Shimizu, K. Otsuka, Int. J. Hydrogen Energy 29 (2004) 1065–1073.
[32] K.C. Patil, S.T. Aruna, T. Mimani, Curr. Opin. Solid State Mater. Sci. 6 (2002) 507–512.
[33] S. Specchia, C. Galletti, V. Specchia, Stud. Surf. Sci. Catal. 175 (2010) 59–67.
[34] L.V. Interrante, M.J. Hampden-Smith, Chemistry of Advanced Materials: An Overview, Wiley-VCH, New York, 1998.
[35] P. Panagiotopoulou, D.I. Kondarides, X.E. Verykios, Appl. Catal. B: Environ. 88 (2009) 470–478.